P2.10: Dual PARG/TOP1 Inhibition Exacerbates DNA-Protein Crosslinks and Replication Stress: A Promising Strategy for Enhancing TOP1i-ADC Efficacy

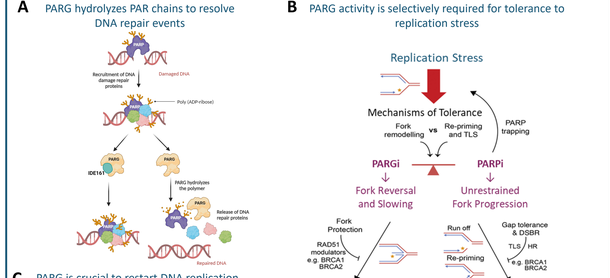
Reeja Maskey, Pei Xin Lim, Megan Conway, Vidhya Nagarajan, Zabrisky Roland, Arjun A. Rao, Ivan Shabalin, Kelly Trego, Jonathon Ryan, Rebeca M. Choy, Peter Teriete, Christian Frey, Yuchen Bai, Paul A. Barsanti, Claire Neilan, Jasgit Sachdev, Michael A. White and Diana M. Munoz
IDEAYA Biosciences, 5000 Shoreline Court Suite 300, South San Francisco, CA 94080, USA

IASLC 2025 World Conference on Lung Cancer
SEPTEMBER 6-9, 2025
BARCELONA, SPAIN

Summary

- Antibody-drug conjugates(ADCs) carrying topoisomerase I inhibitor payloads (TOP1i-ADCs) are having a significant impact as cancer therapies in select tumor types. However, broader use is limited by suboptimal tumor-specific delivery, driven by low or heterogeneous expression of target antigens.
- IDE161 is a potent, orally bioavailable, small molecule inhibitor of Poly (ADP-Ribose) glycohydrolase (PARG), a critical DNA damage response enzyme involved in replication fork restart via hydrolysis of poly (ADP-ribose) (PAR) chains, with potential as an anti-cancer therapy in biomarker defined patient populations.
- Recent findings indicate a critical role for PARG in repairing TOP1-DNA cleavage complexes (Top1ccs), a type of enzymatic DNA-protein crosslink (DPC) that can promote lethal DNA damage when stabilized by Top1i.
- We evaluated the potential for PARG inhibition to selectively amplify TOP1i-induced DNA damage and promote the therapeutic effects of TOP1i-ADCs in multiple preclinical models. We find that the clinical-stage PARG inhibitor, IDE161, significantly enhances TOP1i-dependent accumulation of Top1ccs and associated replication fork failure in cell line models.
- Notably, IDE161 substantially enhances the anti-tumor activity of TOP1i-ADCs, including the clinical DLL3-ADC, IDE849, in both SCLC and low antigen-expressing NSCLC models.

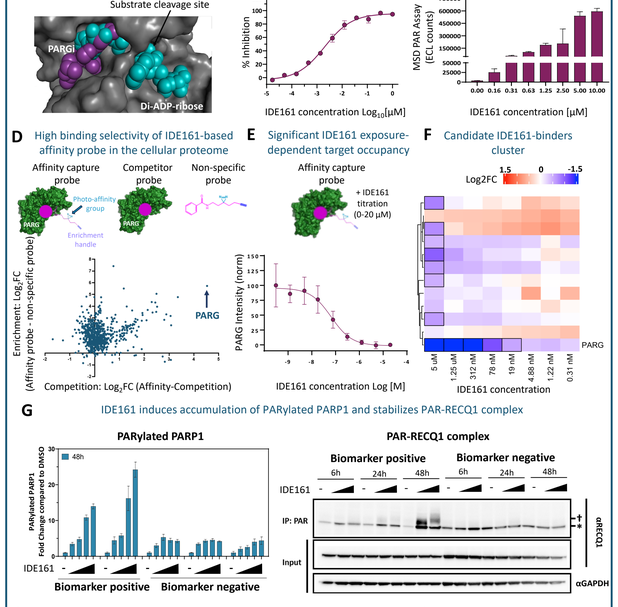
Fig 1. PARG activity resolves PARP-initiated DNA repair complexes to support stalled replication fork stability and restart



Schematics modified from Pillay et al., Progress in Biophysics and Molecular Biology (2021) and Pillay et al. Cancer Cell (2019)

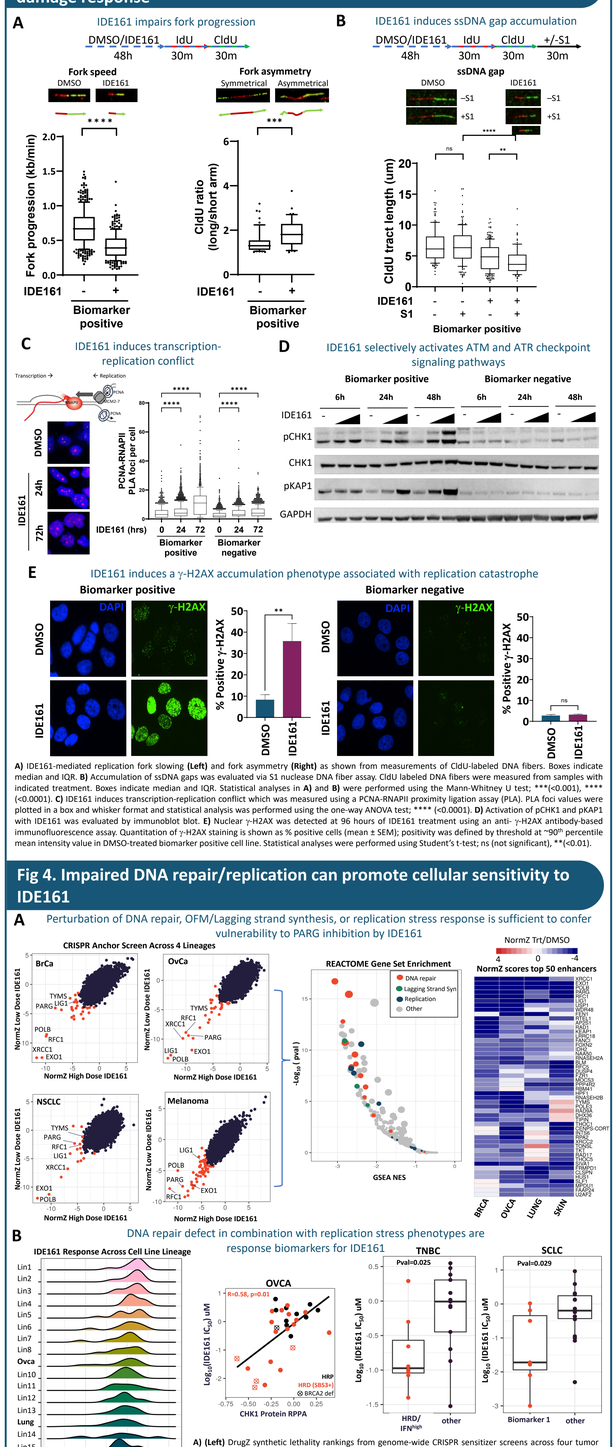
A) Schematic representation of the PARylation process and the effect of PARG inhibition on PAR chain accumulation and DNA repair deficiency. **B)** The diverging effects of PARG versus PARP inhibition. **C)** Other than DNA repair, PARG plays a role at stalled DNA replication forks by regulating RECQ1 helicase for fork restart.

Fig 2. IDE161 is a potent, First-in-Class Phase 1 PARG inhibitor with highly selective target binding profile



A) Overlays of X-ray co-crystal structure of IDE161 (purple) bound to PARG (grey) and Di-ADP-ribose (cyan). **B)** Biochemical potency of IDE161 against human PARG. **C)** PAR chain accumulation assessed via MSD-based PAR assay in a gastric HRD line. **D)** Cellular target engagement assay schema and plot of distinct proteins selectively enriched from whole cell lysates using an IDE161-similar capture probe. **E)** Target occupancy determination and plot of PARG intensity after affinity capture in the presence of increasing concentrations of IDE161. **F)** Heatmap of log2FC of proteins tagged with capture probe in the presence of indicated IDE161 concentrations vs. DMSO control. Proteins with ≥ 0.9 Kendall correlation to PARG are depicted, and contrasts with Empirical Bayes moderated p-value < 0.05 are highlighted with a black box. **G) (Left)** IDE161-mediated accumulation of PARylated PARP1 was measured at 48h using an MSD-based assay. Values are plotted as mean ± SEM. **(Right)** Accumulation of PARylated RECQ1 was measured using an anti-PAR immunoprecipitation (IP) assay. Input and IP samples were evaluated with anti-RECQ1 antibody by immunoblot. *Unmodified RECQ1, presumably pulled down in complex with PARylated PARP1 (not shown). ǂPARylated RECQ1 in direct interaction with PAR antibody.

Fig 3. IDE161 selectively induces replication fork stalling, TRCs and DNA damage response

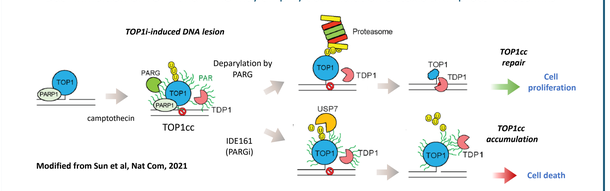


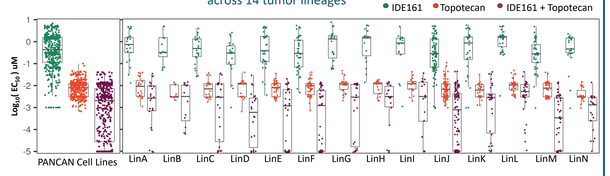
A) IDE161-mediated replication fork slowing **(Left)** and fork asymmetry **(Right)** as shown from measurements of CldU-labeled DNA fibers. Boxes indicate median and IQR. **B)** Accumulation of ssDNA gaps was evaluated via S1 nuclease DNA fiber assay. CldU labeled DNA fibers were measured from samples with indicated treatment. Boxes indicate median and IQR. Statistical analyses in **A)** and **B)** were performed using the Mann-Whitney U test; ***(<0.001), **** (<0.0001). **C)** IDE161 induces transcription-replication conflict which was measured using a PCNA-RNAPII proximity ligation assay (PLA). PLA foci values were plotted in a box and whisker format and statistical analysis was performed using the one-way ANOVA test; **** (<0.0001). **D)** Activation of pCHK1 and pKAP1 with IDE161 was evaluated by immunoblot blot. **E)** Nuclear γ-H2AX was detected at 96 hours of IDE161 treatment using an anti- γ-H2AX antibody-based immunofluorescence assay. Quantitation of γ-H2AX staining is shown as % positive cells (mean ± SEM); positivity was defined by threshold at ~90th percentile mean intensity value in DMSO-treated biomarker positive cell line. Statistical analyses were performed using Student's t-test; ns (not significant), **(<0.01).

Fig 4. Impaired DNA repair/replication can promote cellular sensitivity to IDE161

A) (Left) DruZ synthetic lethality rankings from genome-wide CRISPR sensitizer screens across four tumor lineages at IC_{50} and IC_{90} doses of IDE161. Orange points represent genes with FDR <0.05. **(Middle)** GSEA analysis of NormZ scores, from combined treated compared to combined DMSO samples, in REACTOME gene sets. Point size proportional to number of significantly differentially depleted genes in the leading edge, point color corresponds to the classification of GSEA pathway. **(Right)** Heatmap of NormZ scores of top 50 synthetic lethal genes in IC_{90}dose IDE161 treated versus DMSO **B)** Response to IDE161 across lineages ordered by median IC_{50}. **(Right)** Biomarkers of top responsive lineages are defects in DNA repair and replication stress. OVCA and TNBC HRD were called using SigMA (Gulhan et. al 2019)

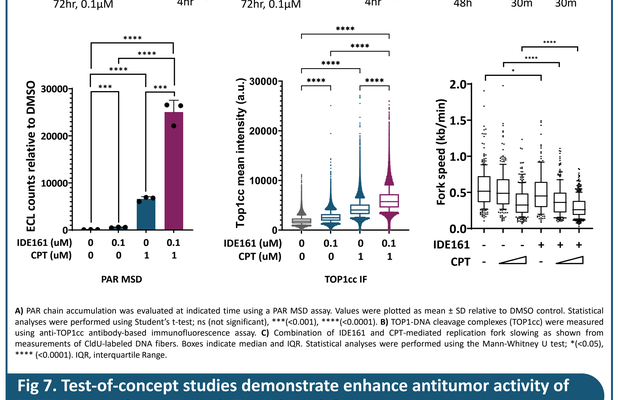
Fig 5. IDE161 and topotecan combination reveals enhanced cytotoxicity in select tumor lineages





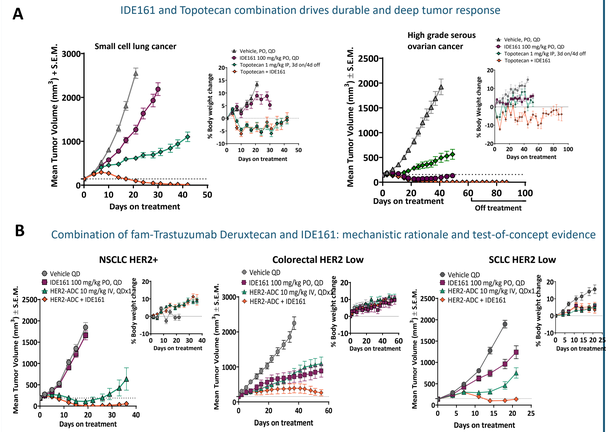
A) Model depicting proposed MOA for dual inhibition of TOP1 and PARG. **B) Left)** Pan-cancer response in PRISM multiplexed cell viability screen for compounds IDE161, topotecan, and IDE161/topotecan combination in 433 cancer cell lines, point color corresponds to the compound treatment for each screen. **Right)** Individual lineage response to single compound, and IDE161/topotecan combination treatment. For combination screening a fixed dose of IDE161 was used in combination with 5-point dose response of topotecan.

Fig 6. IDE161 exacerbates TOP1i-dependent accumulation of Top1cc and associated inhibiton of replication fork progression



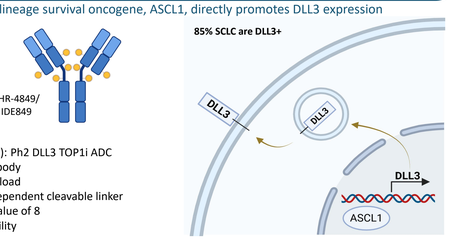
A) PAR chain accumulation was evaluated at indicated time using a PAR MSD assay. Values were plotted as mean ± SD relative to DMSO control. Statistical analyses were performed using Student's t-test; ns (not significant), ***(<0.001), ****(<0.0001). **B)** TOP1-DNA cleavage complexes (TOP1cc) were measured using anti-TOP1cc antibody-based immunofluorescence assay. **C)** Combination of IDE161 and CPT-mediated replication fork slowing as shown from measurements of CldU-labeled DNA fibers. Boxes indicate median and IQR. Statistical analyses were performed using the Mann-Whitney U test; *(<0.05), **** (<0.0001). IQR, interquartile Range.

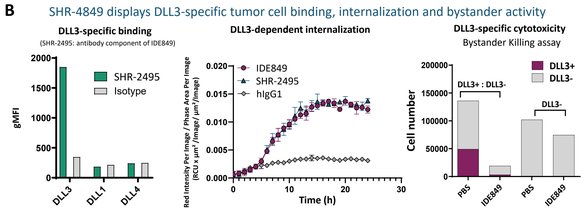
Fig 7. Test-of-concept studies demonstrate enhance antitumor activity of IDE161 in combination with Top1i-based therapies

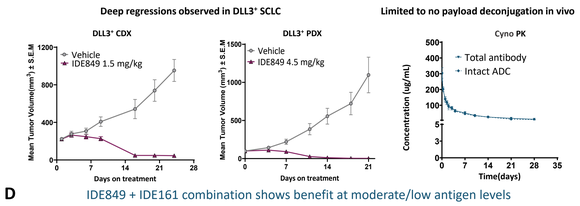


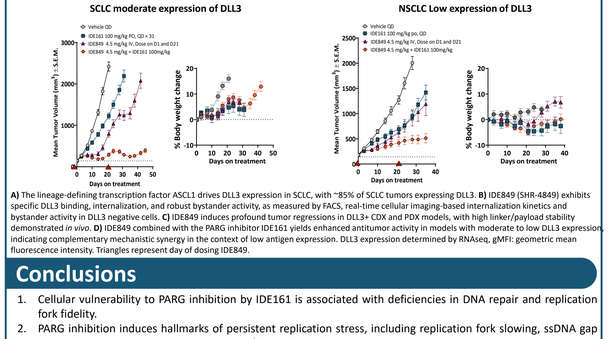
A) In vivo efficacy of IDE161 combined with topotecan shows deep and durable tumor regressions compared to monotherapies. **B)** Co-treatment with fam-trastuzumab deruxtecan (T-DXd) and IDE161 results in enhanced tumor control, supporting a mechanistic rationale and test-of-concept for combining IDE161 with Top1i payload-based ADCs.

Fig 8. IDE849 (SHR-4849): clinical TOP1i-ADC and PARGi combination opportunities







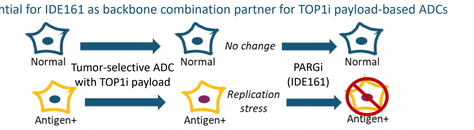


A) The lineage-defining transcription factor ASCL1 drives DLL3 expression in SCLC, with ~85% of SCLC tumors expressing DLL3. **B)** IDE849 (SHR-4849) exhibits specific DLL3 binding, internalization, and robust bystander activity, as measured by FACS, real-time cellular imaging-based internalization kinetics and bystander activity in DLL3 negative cells. **C)** IDE849 induces profound tumor regressions in DLL3+ CDX and PDX models, with high linker/payload stability demonstrated *in vivo*. **D)** IDE849 combined with the PARG inhibitor IDE161 yields enhanced antitumor activity in models with moderate to low DLL3 expression, indicating complementary mechanistic synergy in the context of low antigen expression. DLL3 expression determined by RNAseq, gMFI: geometric mean fluorescence intensity. Triangles represent day of dosing IDE849.

Conclusions

1. Cellular vulnerability to PARG inhibition by IDE161 is associated with deficiencies in DNA repair and replication fork fidelity.
2. PARG inhibition induces hallmarks of persistent replication stress, including replication fork slowing, ssDNA gap accumulation, transcription-replication conflict and ATR checkpoint activation .
3. Context-dependent replication fork failure in the presence of IDE161 may be a consequence of defective Okazaki fragment processing, unresolved transcription-replication conflicts and/or compromised replication fork restart. These events lead to replication fork collapse and cell death.
4. IDE161 impairs resolution of TOP1 cleavage complexes (DNA/protein conjugates) to exacerbate TOP1i-induced DNA damage.
5. IDE161/TOP1i synergy can be exploited to enable efficacy for TOP1i-ADCs in models that otherwise fail to respond due to inadequate payload delivery.

Potential for IDE161 as backbone combination partner for TOP1i payload-based ADCs



6. These findings support the rationale for combining DLL3-targeted ADCs with PARG inhibitors to enhance durability of anti-tumor activity and to overcome limitations associated with low antigen expression, providing a mechanistically informed strategy to extend therapeutic benefit across a broader range of DLL3-expressing tumors.

Acknowledgements

- Present and former IDEAYA colleagues for their many contributions
- CRISPR anchor studies were performed by Cellecta, Inc.
- Viability screen studies were performed by WuXi AppTec and Eurofins
- *In vivo* CDX studies were performed at Pharmaron
- High content imaging from Molecular Devices
- Jiangsu Hengrui Pharmaceuticals Co.
- Broad Institute PRISM

References

- Cortes, U. et al. Mol Cell Biol. 2004
- Gao, H. et al. Exp Cell Res., 2007
- Gogola, E. et al. Cancer Cell, 2018
- Pillay et al. Cancer Cell, 2019
- Gulhan, D. et al. Nat. Genet., 2019 (SigMA)
- Colic, M et al. Genome Medicine, 2019
- Pillay, N. et al. Progress in Biophysics and Molecular Biology, 2021
- Sun, Yilun et al. Nat Comm., 2021
- Cybulla , E et al. Nat Reviews Cancer, 2023
- Ragu, S et al. Genes, 2020
- Pillich RT, et al. Bioinformatics, 2023
- Schaefer, CF. et al. Nucleic Acids Res., 2009
- Harrison D. et al. Front. Mol. Biosci., 2020